Report No. 747

HYDRAULIC PERFORMANCE OF STRUCTURES FOR BRIDGE DRAINAGE

S. C. Kranc, Ph.D., P.E.
Principal Investigator
with
Frank Romano
and
Eric Droz, Richard Deavers, Joshua Wilmot, Scott Eithier, and Guy Rabens

The Department of Civil and Environmental Engineering
College of Engineering
University of South Florida
Tampa, Florida, 33620
Ph. (813) 974-5821

FINAL REPORT
March, 1997

prepared for the
FLORIDA DEPARTMENT OF TRANSPORTATION
and the
U.S. DEPARTMENT OF TRANSPORTATION
FEDERAL HIGHWAY ADMINISTRATION

Technical Report Documentation Page

1. Report No.	2. Government Accession No.	3. Recipient's Catalog No.
747		

4. Title and Subtitle

HYDRAULIC PERFORMANCE OF STRUCTURES FOR BRIDGE DRAINAGE

5. Report Date

July 1997

6. Performing Organization Code

8. Performing Organization Report No.

7. Authors

Kranc, S. C., Romano, F., Droz, E., R. Deavers, J. Wilmot, Ethier, S., and Guy Rabens.

9. Performing Organization Name and Address

Department of Civil and Environmental Engineering
University of South Florida
Tampa, FL 33620-0450

10. Work Unit No. (TRAIS)

11. Contract or Grant No.

BA 034

13. Type of Report and Period Covered

Final Report
October, 1995 - May, 1997

12. Sponsoring Agency Name and Address

Florida Department of Transportation
Office of Research Management
Tallahassee, FL 32399-0450

14. Sponsoring Agency Code

15. Supplementary Notes

Prepared in cooperation with the Federal Highway Administration.

16. Abstract

An experimental investigation of the hydraulic characteristics of temporary concrete barriers employed as inertial attenuators is reported here. Small cutouts are incorporated in the bottoms of the barriers so that a rectangular drainage inlet is formed when the barrier is placed on the pavement. While runoff flow to the channel created by the barrier wall is usually a continuous distribution, the inlets are located at regular, closely spaced intervals, forming discrete drains.

Experimental measurements of the discharge characteristics of various aperture configurations were measured both under sump and transverse flow conditions. Full scale configurations for drainage apertures were tested in an experimental flume with variable cross and longitudinal slope. The results obtained from these measurements were compared wherever possible to existing information. Finally, the information gathered was combined into a predictive model and test cases are presented.

17. Key Words	18. Distribution Statement
Bridge Drainage Inlets	

19. Security Classif.(of this report)	20. Security Classif. (of this page)	21. No. of Pages	22. Price
Unclassified	Unclassified	32	

Form DOT F 1700.7 (8-72)

HYDRAULIC PERFORMANCE OF STRUCTURES FOR BRIDGE DRAINAGE

S. C. Kranc, Ph.D., P.E.
Principal Investigator

The Department of Civil Engineering and Mechanics
College of Engineering
University of South Florida
Tampa, Florida, 33620
March, 1997

TABLE OF CONTENTS

CONVERSION FACTORS

To convert	British	SI	multiply by
Acceleration	ft/s^2	m/s^2	3.048E-1
Area	ft^2	m^2	9.290E-2
Density	$slugs/ft^3$	kg/m^3	5.154E+2
Length	ft	m	3.048E-1
Pressure	lb/ft^2	N/m^2	4.788E+1
Velocity	ft/s	m/s	3.048E-1
Volume flowrate	ft^3/s	m^3/s	2.832E-2

NOTATION

a= constant, Eq. 21

a_i= empirical constants

A= area of flow

b= length of barrier block

b_s= spacing between inlets along a barrier wall

B= width of barrier block

Cd= discharge coefficient

E= efficiency

Fr= Froude number

g= acceleration of gravity

h= depth of flow

H= height of opening

k= constant in Manning's equation

k_1= constant, Eq. 14

k_2= constant, Eq. 15

l= spread measured across pavement

L= width of opening

L_h= length along pavement

L_s= length along pavement

L_T= capture length

n= Manning's n

q_{ro}= runoff flowrate per unit length

Q= flowrate

Q_{co}= carryover flowrate

Q_{ro}= runoff flowrate

Q_i= flowrate through inlet

Q_s= initial flowrate

Q_1= flowrate upstream

Q_2= flowrate downstream

R= hydraulic radius

S_c= cross slope

S_0= longitudinal slope

S_f= friction slope

T= spread

V= velocity of flow

W_p= pavement width

x = distance variable along pavement

y= depth of flow measured against barrier block

y_1= depth upstream of inlet

y_2= depth downstream of inlet

EXECUTIVE SUMMARY

Temporary concrete barriers are often employed in highway construction projects (FDOT INDEX 415[1]) as inertial attenuators. Because of concerns for adequate pavement drainage, small cutouts are incorporated in the bottoms of the barriers so that a rectangular drainage inlet is formed when the barrier is placed on the pavement. While runoff flow to the channel created by the barrier wall is usually a continuous distribution, the inlets are located at regular, closely spaced intervals. In this regard, the arrangement of inlets is much like a manifold problem.

The purpose of the present investigation is to develop a method for estimating total drainage associated with a line of barriers. To accomplish this goal, experimental measurements of the discharge characteristics of various aperture configurations were measured both under sump and transverse flow conditions. Various full scale configurations for drainage apertures were tested in an experimental facility consisting of a tilting flume, circulating pumps and a large reservoir tank. Water was withdrawn from the reservoir, pumped to the flume bed then exited the flume, either by the drain or at the termination of the channel to drop to the reservoir below. Both the cross and longitudinal slope of the flume could be varied, with zero longitudinal slope corresponding to sump conditions (no channel velocity). The results obtained from these measurements were compared wherever possible to existing information. Finally, the information gathered was combined in a predictive model and test cases are presented. Application methods are suggested.

INTRODUCTION

During roadway construction projects, temporary barrier walls made of precast concrete blocks are set along highways and bridges to provide lane and side protection for the flow of traffic as shown in Figure 1 (Index 415[1]). Because these barrier blocks rest directly on the pavement or shoulder, a hydraulic configuration much like a curb and gutter is created. During rainstorms, water runoff from the pavement accumulates along the side and flows along the barrier wall at a rate which depends in part on factors such as roughness and slope of the roadway. At bridge approaches a similar configuration is permanently installed for sidewalk drainage (Index 410[1]).

Providing adequate drainage for these temporary barriers is a complex issue. Typically, each concrete barrier section is formed with one or two cutouts to allow for drainage underneath. As originally formed, the drain aperture is rectangular in cross section much like a side inlet (to avoid confusion, these drains will be referred to as "inlets"). The problem is similar in some respects to conventional curb drainage, ie. a triangular shaped channel with drain apertures located at regularly spaced intervals. However, temporary barriers are fitted with closely spaced openings, and it is possible that uniform flow does not develop between the openings, due to the short reach. Consequently, from a hydraulic viewpoint the problem also resembles a trough with continuous inflow (from pavement drainage) and outflow at intervals along the pavement. In this regard, the arrangement of inlets is a manifold problem similar to that encountered in irrigation applications[2,3]. Furthermore, because the shape of the drainage aperture is a simple rectangle, flush with the adjacent pavement, none of the improved flow characteristics normally associated with a depressed inlet will be attainable. While the edges are formed to be square, field observation indicates that the edges are often chipped so that the actual shape is more nearly a rough beveled or round. Finally, the conditions at the outlet end of this channel cannot be stated with certainty; the pavement may continue as a flat surface or a sudden drop off may occur.

The purpose of the present investigation is to develop a procedure for estimating drainage through the array of openings in these temporary barrier structures. In contrast to permanent installations where the spacing and size may be adjusted at the design stage, the task here is to determine capacity of the barrier wall system, since the size and location of the openings are fixed. To accomplish this task, information regarding the flow capacity of the individual inlets is required. Ultimately the significance of this problem is safety; adequate drainage must be provided for the maximum anticipated storm event so that the spread of water flowing along the barrier does not impinge on the adjacent traffic lane, which in many construction situations may be quite close to the wall.

HYDROLOGY OF PAVEMENT DRAINAGE

Methods for calculating the hydraulic load accumulated on pavement and runoff to the curb are presented elsewhere[4,5], and the discussion presented here will be restricted to the hydraulics of the channel and drain inlets. It is expected that the normal hydraulic load of water accumulating at the barrier is simply runoff from the pavement (computed by conventional methods), although the possibility of an initial flow of water at the beginning of the barrier line carried over from locations up grade from the barriers must also be considered.

ANALYSIS OF THE SIDE CHANNEL FLOW

The problem of gutter flows has been extensively investigated and most of the current design philosophy is summarized elsewhere[4,5]. For purposes of the present discussion, a simplified picture of the curb/gutter geometry formed by temporary barrier structures can be adopted. Because the concrete barriers rest directly on the pavement, the vertical edge of the barrier is normal to the paved surface. Thus the

channel formed is then a right triangle, and the spread on the pavement is simply related to the cross slope as shown in Figure 2. The drain aperture in the barrier forms a side opening inlet in the curb wall and flow through the inlets in the temporary barrier is along the same slope as the pavement (in the case of sidewalk drainage slots provided in permanent barrier walls, the slope is much greater). Although it would be expected that the hydraulic performance of the inlet is closely related to that of conventional curb opening inlets, some differences are anticipated due to the short length of the opening.

The pavement has cross slope S_c and longitudinal S_0. Assuming the barrier forms a 90° angle with the pavement, a triangular section is formed with depth h. Because the cross slope is a small angle, the spread is approximately the same as the length across the pavement and the depth h, is very close to the measurement y, against the barrier, as seen in the figure. These two approximations will be used throughout the rest of this report. Thus, the spread is approximately

$$T \approx \frac{y}{S_c} \tag{1}$$

The area is given approximately as

$$A \approx \frac{y^2}{2S_c} \tag{2}$$

The hydraulic radius becomes

$$R_h \approx \frac{y}{2} \tag{3}$$

The flow velocity may be obtained from continuity

$$V \approx \frac{2QS_c}{y^2} \tag{4}$$

The Froude number is defined in terms of the average depth

$$Fr \approx \left(\frac{8}{g}\right)^{1/2} \frac{QS_c}{y^{5/2}} \tag{5}$$

The critical depth is

$$y_c \approx \left[\frac{8Q^2S_c^2}{g}\right]^{1/5} \tag{6}$$

The specific energy becomes

$$E \approx y + \frac{2Q^2S_c^2}{gy^4} \tag{7}$$

Utilizing Manning's equation formulated for a triangular channel

$$Q \approx \frac{kS_0^{1/2}y^{8/3}}{2^{5/3}nS_c} \tag{8}$$

Here, k is the constant associated with Manning's equation (1 in SI units, 1.485 in the English system). This equation can be solved for the normal depth

$$y_n \approx 2^{5/8}\left[\frac{QS_cn}{kS_0^{.5}}\right]^{3/8} \tag{9}$$

It is often suggested[4], however, that because the surface width of the flow is very large in comparison to depth, the standard formulation for a channel of triangular cross section is not completely satisfactory for predicting flow conditions and experimental evidence appears to confirm this discrepancy. An alternative formulation has been developed by integrating Manning's equation for infinitesimal rectangular elements of variable depth across the channel width, giving

$$Q \approx \frac{3kS_c^{5/3}S_0^{1/2}T^{8/3}}{8n} \tag{10}$$

This formula, which will be used throughout the remainder of this report, yields results about 20% higher for the flow rate than that predicted by Equation 8. The normal depth associated with Equation 10 is

$$y_n \approx \left[\frac{8QS_cn}{3kS_0^{1/2}}\right]^{3/8} \tag{11}$$

The derivation presented above is typical of the approach used to analyze curb inlet flow problems. Because the spacing between inlets is small it cannot be assumed that the flow is at normal depth as is done in the case of permanent inlets in curbs. The situation for barrier drains requires some modification, primarily to account for multiple, closely spaced inlets, but also the inflow runoff from the pavement.

PERFORMANCE OF INDIVIDUAL INLETS

As is evident from the discussion above, information concerning the discharge characteristics of the barrier inlets is required if computation of the capacity of a barrier system and pavement spread during a storm event is to be attempted. It can be anticipated that the flow through the inlet will depend on several factors including inlet shape, cross slope, velocity past the inlet face as well as depth of the channel flow adjacent to inlet. While the pavement surface and the barrier face have associated

roughness, it is not necessary to independently investigate this parameter (bed roughness will be a factor in computations of channel flow, however). To maintain a tractable approach to this problem, additional simplifications will be introduced as follows:

1. It is assumed that no interference between adjacent inlets occurs, so that isolated inlets have the same performance as closely spaced inlets.

2. The effect of irregularities in the channel flow on the performance of the inlets is ignored.

3. The effect of other openings, such as the spaces between the adjacent barrier blocks and leakage between the block and pavement is ignored.

4. Each inlet is clear of trash and debris.

5. Under some conditions a hydraulic jump might form at the inlet, as the channel flow makes a transition from a supercritical to a subcritical flow. This special case is not considered.

6. The flow passage under the barrier is so short that roughness in this section is not expected to be an important factor in determining flow capacity of the inlet.

The overall performance of an inlet may be subdivided into two important cases of interest. The first of these is concerned with the performance when the water upstream of the inlet is stagnant (sump condition), or has a low velocity past the inlet face. This situation is analogous to any aperture flow from a large reservoir. It is customary to measure the reservoir elevation and to use this parameter to correlate the performance. For several reasons, in the present investigation this choice is not

practical and instead a measurement of water depth at the side of the inlet will be taken instead, as explained in more detail later.

It can be expected that the opening will have a characteristic discharge-depth relationship with different flow regimes as shown schematically in Figure 3. At least three modes of operation can be identified. 1) for $y<1.4H$, a weir flow through the opening 2) for $y>1.4H$, an orifice type model, and 3) for $y>>H$ a nozzle like mode with the entire passage filled with liquid will develop. It is also possible that some unstable flow regimes may develop in transition regions.

The second case involves substantial flow past the face of the inlet as would occur on a longitudinal slope. Depending on conditions, this flow might be either supercritical or subcritical. If the velocity is substantial, the flow patterns around the inlet will be altered from the sump condition, and a reduction in capacity is to be expected. The flow through an individual inlet, will be denoted Q_i and the flow in the main channel upstream and downstream will be denoted Q_1 and Q_2 respectively. In some cases of very low flow, total capture at the inlet may be possible. More often however, some fraction of the flow will bypass the inlet and continue in the main channel. It is convenient to define an efficiency of capture as the ratio of inlet flow to approaching flow ($E=Q_i/Q_1$).

EXPERIMENTAL FACILITY AND OBSERVATIONAL METHODS

Experiments reported here were performed at the Hydraulics Research Lab at the University of South Florida in Tampa. The facility (Figure 4) was reconfigured in the following manner for the purposes of these tests. A tilting bed was constructed and placed over a large fiberglass reservoir tank. Both cross and longitudinal slope could be varied in this manner, using a long level to set the desired value. Water was supplied to the bed by up to three centrifugal pumps through lines fitted with

paddlewheel type flow meters for measurements. After passing over the bed and through the inlet, water was returned to the reservoir.

Two types of experiments were conducted, one being tests with no approach velocity designed to simulate sump conditions at the inlet, and the other with velocity past the inlet to simulate barriers on grade. In the first case water was distributed through a baffling manifold, evenly across the bed which was set at zero longitudinal slope. In the latter case an approach trough 5.6 m in length was constructed with the pumps discharging at the upper end.

Models of the temporary barrier drains were constructed to full scale from resin coated plywood. For the model tests conducted here, the effect of surface roughness was not independently investigated. This construction resulted in a relatively smooth surface. Two aperture widths of 762 mm (2.5 ft) and 152 mm (0.5 ft) were used. In both cases the aperture height was 51 mm (0.17 ft) and the dimension through the barrier in the direction of flow was 610 mm (2.0 ft). Both square edged and an edge rounded to a 38 mm radius was used (only the vertical edge was rounded). For most tests, the flow made a free overfall at the outer edge of the barrier. Several tests were made with an extended base but this condition seemed not to be influential and was discontinued.

Due to capacity limitations of the system it was not possible to produce a full flow in a triangular channel for tests with flow past the inlet face. Instead a second barrier wall was placed 300 mm away from the wall to form a trapezoidal channel. It was assumed that placing the wall at this position caused no distortion to the main body of the flow and that the inlet flow was identical to that which would have been produced in a triangular channel.

For measurement of inlet flow under sump conditions, the pump discharge measurements (paddlewheel type flow meters) could be used directly. Measurement of

flow through the aperture under non sump conditions was accomplished by capturing the flow, which was then routed through a separate line with another paddle wheel indicator. A butterfly valve at the end of this line was used to throttle the discharge so that full flow in the line was ensured. For calibration, the output of this paddle wheel was correlated with the discharge line from the pumps when all flow was routed through the line.

Measurement of the flow depth was accomplished by direct measurement of the surface elevation. A jig straddling the test section was used to provide a datum and a sharp tipped ruler was used to locate the surface. Surface and bed elevations were measured at five stations across the channel with this arrangement. The station located closest to the side was not positioned directly at the wall but rather at 25mm away, to avoid a surface wave. The water depth was then calculated by extrapolating to the depth at the wall. The area was calculated from an average of all points and the velocity was then calculated from this measurement and the flow rate.

EXPERIMENTAL RESULTS

Sump conditions

An extensive series of tests were conducted under sump conditions. The performance of both inlet sizes has been summarized as a head-discharge diagram (Figure 5). The data follow the typical performance characteristics for an aperture, exhibiting a regime of weir flow for the lowest heads, then developing an orifice type flow as the free streamline touches the top of the opening. It was observed that for the highest heads operation with the flow completely filling the inlet channel could occur. Thus the performance is analogous to that encountered for culvert operation.

For convenient representation, data for both aperture widths were correlated with

cubic polynomials by multiple linear regression. Only sharp edged openings were included in the correlations and all slopes were grouped together. A comparison between the data and the correlations are shown in Figure 5. While the data for the smaller opening could be represented by a single equation, the larger opening required two separate relationships for different regimes. It was determined that the flow is a direct function of width, as would be expected. The correlations were then rescaled to the standard widths described in Index 415 by multiplying each coefficient by the ratio of the standard width to the model width, and the results are presented in Table 1. Prediction of the flow in the region between weir and orifice control for the larger opening may be predicted by extrapolating the orifice equation.

It should be noted that a single barrier block with one long opening (790 mm) has a capacity exceeding that of a barrier block with 2 shorter openings (each 150 mm). For example, at sump conditions at a head of 120 mm, the difference in capacity is a factor of about 2.5.

Flow past the opening

The second major concern was the performance of the inlets under conditions of flow past the inlet face. Due to experimental limitations, it was not possible to independently vary velocity and depth for a particular cross slope condition as would be desirable. Rather it was necessary to accumulate a data set over a limited head range and deduce the velocity. To place the data in a suitable context for interpretation and application, several different correlations were attempted. As illustrated in Figure 6 it was found that simply plotting the data as a function of depth, again measured at a point just upstream of the entrance, was found to be most straightforward. It should be understood that this step represents a substantial simplification, and does not imply that velocity past the face or cross slope are not important overall performance factors. Interpretation of the influence of velocity on interception characteristics is more complex. Only a limited amount of data for subcritical flow past the inlet was obtained

and this data indicated only slightly different results from sump conditions (for comparison, empirical fits to sump conditions have also been plotted). Once the flow achieves a supercritical condition, a more substantial reduction in performance was observed, but little dependence on velocity under this condition was noted over the range of parameters examined here.

For application purposes, this data was treated in the same manner as that described for data taken under sump conditions. To examine the importance of cross slope, the data were grouped, with S_c = 0.0 and 0.02 as one group ("small") and S_c=0.08 and 0.1 as another ("large"). A linear fit was judged sufficiently accurate for representation as shown in Figure 6, and little independent influence with cross slope could be detected. To obtain the best fit, it was necessary to include an intercept in the data for the smaller openings. It should also be noted that the data for the smaller openings includes two extra data sets, one set (open inverted triangles in Figure 6) represents data taken under subcritical conditions and correlates more closely with sump conditions. The second set (inverted "Y") represents data for which calibration of the flow measurement was questionable. Neither of these sets were incorporated into the fitting procedure.

Again, for presentation in Table 1, it was necessary to rescale the data as discussed previously. In contrast to the sump data however, it was found that the flow was not a direct function of aperture width, ie. while the large aperture is about five times larger than the small aperture, the capacity of the larger is substantially less than five times as great. While small adjustments to different widths are reasonable extrapolations, attempts to project performance for substantial differences in width should be undertaken cautiously.

Table 1: Empirical coefficients for discharge relationships. Note that both SI and (English) units are provided. The variable y should be in meters or feet.

Sump conditions: constants for the cubic relationship $Q(y)=a_1+a_2y+a_3y^2+a_4y^3$

Case	a_1	a_2	a_3	a_4	range (y/H)
L=150 mm	0.0	0.041 (0.44)	0.11 (0.35)	-0.57 (-0.57)	0.0-3.6
L=790 mm	0.0	0.196 (2.11)	-5.03 (-16.51)	3.00 (83.0)	0.0-1.4
L=790 mm	0.0	0.415 (4.47)	-1.97 (-6.47)	4.43 (4.43)	1.4-3.6

Flow past face: constants for the linear relationship $Q(y)= a_1+a_2y$

Case	a_1	a_2	range (y/H)
L=150 mm	-4.5×10^{-4}(-.016)	.0375(.404)	0.25-3.25
L=790 mm	0.0	.114(1.23)	0.00-2.00

DISCUSSION

Sump conditions

The head-discharge relationship for flow through apertures can often be expressed in terms of a non dimensional discharge coefficient. For weir flow

$$Q = C_D L\sqrt{2g}\, y^{3/2} \qquad (12)$$

For orifice and nozzle type flows

$$Q = C_D A\sqrt{2g}\,(y-\frac{H}{2})^{1/2} \qquad (13)$$

In the present investigation, correlations for orifice and nozzle type flows were made using the depth to the centroid of the opening[4], where y is measured at the side wall, as explained previously. Equation 12 was used for y<1.4H and Equation 13 for y>1.4H.

It can be seen (Figure 7) that data sets for both openings can be brought together by these correlations indicating that both sizes tested have comparable efficiency under sump conditions. Again, the general trend of the discharge coefficient is consistent with that observed for aperture flows. For higher heads, the discharge coefficient is constant and close to 0.5, as would be expected for an orifice. When the edges of the aperture are rounded, a much higher value for the discharge coefficient is obtained.

Values for the discharge coefficient suggested previously[4] correspond to C_D=0.29 for the weir regime and C_D=0.67 for orifice flows, respectively. It is evident that the discharge coefficient calculated for the results of the present investigation are not constant in the weir regime, but vary considerably, especially at low heads. This observation is consistent with typical broad crested weir behavior, resulting from the combined effects of separation at sharp edges and boundary layer growth. In the orifice regime, the discharge coefficient is lower than the 0.67 value for most cases except those with rounded edges. As expected, it can be seen from inspection of the data that a modest improvement results from rounding the sides of the inlet entrance. Most discrepancies between the results reported here and other studies are likely due to configurational differences and the effect of scale.

Flow past the opening

Side opening inlets have been investigated extensively because of common

application to pavement drainage, and this configuration is perhaps the closest analogy to the barrier aperture studied here. An empirical equation describing performance has been given[4], relating the length of drain face opening, L_T, required to accommodate a flow Q.

$$L_T = k_1 Q^{.42} [\frac{S_0^{.5}}{nS_c}]^{.6} \tag{14}$$

Here k_1 is an empirical constant, equal to 0.815 in SI units and 0.6 in English units. Substituting from Equation 10

$$L_T \approx \frac{k_2 Q}{y^{1.6}} \tag{15}$$

where k_2 absorbs all constants (k_2 =3.24 SI, =.852 English). A comparison of the predicted inlet flow, $Q_{i\,pred}$, to that measured in the experiments reported here can be accomplished by computing the efficiency of the inlet. For flows in excess of the capacity of a particular length L, the efficiency $E_{pred}=Q_{i\,pred}/Q$, has been correlated[4] with L_T by

$$E_{pred} = 1-(1-\frac{L}{L_T})^{1.8} \tag{16}$$

Substituting,

$$E_{pred} = 1-(1-\frac{Ly^{1.6}}{k_2 Q})^{1.8} \tag{17}$$

It is noted that slope has been eliminated as a parameter. An efficiency can be deduced from the experimental data by using the observed velocity and the area of the triangular channel (to rescale the data to a channel of full width). Thus

$$E_{exp} \approx \frac{2S_c Q_{i\,exp}}{Vy^2} \qquad (18)$$

A cross plot of the predicted and measured efficiency is presented in Figure 8. Most of the data appear to be scattered around the 45° line, and it appears that these small inlets tested are comparable to the larger inlets for which the correlations were originally developed. While the agreement is reasonable, several cautionary notes are in order. First, no limits of validity are indicated for the correlations utilized here[4]. The configurations tested here are not identical with those used for the correlations, and in particular the overall lengths of the experimental inlets are much shorter. This difference means that the efficiency of the inlets are relatively low.

It is also noted that at the upper right side of the cross plot several points are noticeably shifted away from the 45° line to the right, indicating much poorer agreement with the correlation. In fact, these data were obtained for very high heads, where the inlet is beginning to run full, possibly outside the range of the correlation.

For most situations studied, the flow past the inlet face was supercritical. In many practical applications, subcritical flow will occur only at small longitudinal slope and relatively low velocities, so that the inlet flow will be only slightly less than that predicted for sump conditions. The correlation of Equation 17 could be used to predict flow for low velocity, subcritical situations (or the flow could be estimated from sump conditions). Although this correlation does not have a distinct break between the two regimes, in fact for larger longitudinal slopes (higher velocities) the inlet flow is only a weak function of slope. The experimental results of this investigation indicate that inlet flow is not substantially affected by cross slope as would be expected.

Finally, a possible reason for the improved performance of the smaller aperture over the larger may be as follows. It was observed during tests that a sharp

downstream edge of the inlet produced both a "rooster tail" spray and an oblique hydraulic wave[6], elevating the water depth over part of the entrance. This region also was observed to be the region of largest inlet flow at the outfall. Since the size of this region did not depend on the length of the opening, the smaller inlet was more strongly affected. It should be noted however, that a barrier block having one large inlet has a larger capacity than a block with two of the smaller inlets.

A PREDICTIVE MODEL

A predictive model for the water depth for flow along an array of barrier wall inlets (Figure 9) can now be formulated. As discussed previously, because the spacing between inlets is small it cannot be assumed that the flow is always at normal depth just upstream of the inlet entrance (a tacit assumption for permanent inlets in curbs). Thus, a more detailed analysis of the water depth along the wall allowing for both inflow and outflow (through the inlets) is required.

Numerical solution

Following Henderson[7], the continuous addition of water to the channel (sheet flow from the pavement at a rate dQ_{RO}/dx) is dissipative and adds no momentum to the flow. The specific energy equation is not available for analysis in this case but instead the momentum equation applies

$$\frac{dy}{dx} = \frac{S_0 - S_f - \frac{2Q}{gA^2}\frac{dQ}{dx}}{1 - Fr^2} \tag{19}$$

For the situation of interest here, flow in a triangular channel, Equations 1-7,10,11 are assumed to hold. The "friction" slope, S_f, is conventionally defined as the slope consistent with normal depth for any Q, computed here from Manning's equation (Equation 10). Equation 19 may be used to compute the water elevation along the

channel between the inlets, however it is not a simple matter to generalize the change in water depth in the direction of flow since numerous cases can be identified according to the relative magnitudes of the parameters of this equation.

The inlets may be regarded as discrete discharges, with flow dependent on the elevation of the water before the opening, as discussed previously with regard to the hydraulic performance diagram. Continuity gives the change in flow rate along the channel across the inlet.

$$Q_1 - Q_i(y_i) = Q_2 \tag{20}$$

Here Q_1 is the upstream flow, Q_2 is the downstream flow and Q_i is the flow from an individual opening. It is assumed here that the division of flow causes no loss of specific energy across the inlet[7]. Thus the specific energy equation (Equation 7) may be used to solve for y_2, once Q_2 is known. The resulting equation is

$$ay_2^5 - ay_1y_2^4 - Q_1^2\frac{y_2^4}{y_1^4} + Q_2^2 = 0 \tag{21}$$

where $a=2S_c^2/g$.

The water depth along the wall can be calculated according to the following scheme:

1. An initial flow and corresponding normal depth at the upstream end of the array are assumed to begin the calculations. Starting with a positive value eliminates some complications which would occur if zero flow were assumed. This flow can be relatively small and arbitrary or might account for an actual, substantial flow from another source.

2. A solution to Equation 19 can be developed using an appropriate finite

difference formula (for example, a simple second order Runge-Kutta method) to compute the water depth between successive inlets. Computations should march downstream in relatively small steps.

3. At each inlet the march is halted and the water depth is used to compute the inlet flow Q_i, then Equation 20 is used to calculate the new flow rate just downstream of the inlet. For purposes of this discussion, the empirical correlations from Table 1 will be utilized to determine the flow through any particular orifice.

4. Equation 21 is used to calculate the water depth, y_2, just downstream of the inlet. Newton's iterative scheme may be used to solve this relationship.

5. The results of steps 3 and 4 become the starting condition for the water profile moving towards the next inlet.

Steps 1 to 5 are repeated to the end of the reach. The possibility of a transition to a subcritical condition could be handled in conventional fashion, although this situation is probably not relevant to the present discussion.

Example

An example will help to clarify these points. Suppose the pavement section of interest is 153 m long and configured as follows:

W_p= 10 m (width)

S_c= .02

S_0= .05

n= .016

According to Index 415[1], barrier blocks have a minimum length of 3600 mm. Placed in a line, the space between inlets will then be 2810 mm for the 790 mm inlets. When two 150 mm inlets are used, the space alternates between 1680 and 1620 mm. For the

present example, small inlets (L=150 mm) will be assumed. For simplicity, an average value of b_s= 1650 mm may be used without compromising accuracy.

A storm event is assumed with a precipitation rate P= 2.8×10^{-5}m/s (0.1 m/hr). For simplicity this rate is assumed to be the runoff from the pavement,

$$q_{RO} = PW_p \tag{22}$$

so that $q_{ro}=2.8 \times 10^{-4}$ cubic meters/sec per meter along the wall.

Figure 10 illustrates the solution to Equation 19, for different initial flows. It can be seen that the spread approaches a limiting value of 1.3 m at about 150 m along the wall. An explanation for these results may be found by examining the performance of an individual opening and the accumulation resulting from runoff following the last opening (Figure 11). Although the local runoff accumulated between two adjacent inlets is relatively small, the openings are not long enough for complete capture if the head is low. As the magnitude of the flow builds along the wall, eventually a steady state may be achieved when the depth is sufficient to discharge an amount equal to the accumulation between inlets and both the spread and the depth just before the inlet remain constant. This condition will be referred to as "equilibrium flow", by analogy to uniform flow. The magnitude of this flow is 0.0134 m^3/s, for the example above.

This condition can be further explained by equating the runoff accumulation between openings to the empirical flow relation (Table 1). Solving for the spread gives

$$T = \frac{q_{RO}(b_s+L)-a_1}{a_2 S_c} \tag{23}$$

where the constants a_1 and a_2 represent the appropriate coefficients. Once the spread is known the equilibrium flow can be determined from Equation 10.

Continuing the example above, a_1=-0.00045(m^3/s) and a_2= 0.0375 (m^2/s), obtained from Table 1 and the following may be calculated. The flow through the inlet is $q_{ro}(b_s+L)=5x10^{-4}m^3/s$ and the spread (Equation 23) is T=1.27 m. Assuming uniform conditions, the equilibrium flow along the wall (Equation 10) is $2.6x10^{-3}m^3/s$. As long as conditions remain constant, this equilibrium can be maintained and the main flow along the wall does not vary. Even if the flow is not in a uniform state just before the entrance, similar arguments show that a steady state can result.

An approximate model

The detailed analysis presented above yields complete information about the flow along the barrier wall, including water depth and spread, system capacity, the equilibrium condition and finally the reach necessary to achieve this equilibrium state. Unfortunately, the model presented is complex and difficult to use. A more tractable, approximate model may be formulated by assuming that the flow always returns to a uniform condition just before the inlet (except for the large number of inlets involved, this approach is similar to that used to size curb inlets). This simplification means that the same results can be produced by an elementary spreadsheet calculation as follows. At some point (x=0) an initial flow Q_2 is specified (often zero). A spatial step equal to the spacing between the inlets and the inlet width is made, and the total accumulation is calculated as $P(L+b_s)$. This runoff is added to Q_2 to give the flow just upstream of an inlet, Q_1. The normal depth at this point is calculated from Equation 11. The flow into the inlet is calculated according to Table 1 and the main body of flow, Q_2, just downstream of the inlet is calculated according to Equation 20. The process repeats for as many inlets as are present in the system. A comparison of the two methods is given in Figure 10. The approximate method yields a slightly elevated estimate of main flow along the barrier wall, presumably because the actual depth is slightly larger than the normal depth just upstream of the inlet.

ESTIMATING CAPACITY FOR BARRIER SYSTEMS

A barrier system often comprises an extended line of barrier blocks with several grade changes. As shown in the previous section, the problem of determining the flow on sections of pavement with longitudinal slope can be complex, but essential in determining the carry over onto the horizontal section. Before performing extensive calculations, a simple estimation procedure may be adequate. Specifically:

1. Determine the magnitude of the equilibrium flow on the sloped section. Determine the spread associated with this flow (Equation 23).

2. Assuming supercritical conditions, if the initial flow at the top of the slope is smaller than the equilibrium flow calculated in 1. above, the spread on the sloped section will not be larger than that associated with equilibrium flow. In this case, the magnitude of the carryover to the horizontal section will be no more than the equilibrium flow on the slope.

3. The possibility of a source flow at the beginning of the line of barriers must be considered. If the initial flow is larger than the equilibrium flow, the spread associated with the initial flow will be the largest spread encountered on the slope and this is the also the upper limit for the magnitude the carryover flow.

4. Determine the runoff flow to the horizontal section according to 2. or 3. above.

Inspection of the previous results will serve to illustrate these points. It is emphasized that this scheme is approximate and suggested for the purpose of making an initial estimate. If the spread anywhere along the barrier line calculated by this approximate method exceeds the allowable spread, more extensive calculations, using either the approximate method or the more exact analysis outlined in the previous section may be necessary to determine actual magnitudes.

When considering the drainage of horizontal sections, it will be necessary to combine any residual flows from sloped sections that carry over onto the horizontal section. The spread associated with the combined flow may be according to the scheme outlined below.

Example

As a basis of discussion, an continuation of the example given in the previous section is envisioned (other problems may be addressed by extensions of the methods illustrated here). A section of pavement, L_p=153 m, with zero longitudinal slope is located in a depressed region between two sections of pavement with longitudinal slope, S_0=0.05 and the same length, L_s=153 m as shown in Figure 12. As with the sample computation given in the last section the width of the pavement is 10 m and all sections have cross slope S_c=0.02 towards the side which is lined with temporary barriers. It is desired to ensure that a maximum storm event can be accommodated without excessive spread of water into the traffic lane.

Flow on grade

In this case, the magnitude of this flow is relatively small, Q=0.0134 m^3/s approaching the central section from each side (computed previously) and equal to the accumulation between two adjacent inlets.

Depressed section

The horizontal section is considered next. Water ponding in this depressed area is accumulated as runoff from the adjacent horizontal pavement section and also from the carryover (residual) flow delivered from the sloped sections on either side. The maximum volumetric flow rate (per unit length along the pavement) towards the side due to local runoff, is calculated from the precipitation rate. As before, this rate is q_{ro}=2.8x10^{-4} m^3/s-m. To the local runoff must be added the carryover flow from the sloped sections on either side of the horizontal. In this example the value is Qco=0.027

m^3/s, twice that computed previously to account for both sloped sections. It is assumed that this flow is distributed equally over the entire horizontal section, L_h=153 m. Thus the total flow per inlet becomes

$$Q_{tot} = (q_{ro} + \frac{Q_{co}}{L_h}) \cdot (L + b_s) \qquad (24)$$

Obviously for a quasi-steady condition, flow out must equal flow in and the depth of water at the barrier wall determines the flow out. The experimental relations for sump flow may be reformulated as an empirical relationship for depth as a function of discharge as shown in Table 2. Inserting the value Q_{tot}, and dividing by the slope (Equation 1) yields the spread on the horizontal section. In this case, Q_{tot} =8.22x10^{-4} m^3/s and T= 0.96 m, less than the maximum spread on the sloped section (1.27m), due to the improvement in performance under sump conditions. If this spread is within tolerable limits, then the drainage provided by the barrier openings is adequate. It should be noted that the relationships in Table 2 cannot be easily extrapolated to other aperture widths. If required this information can be obtained by directly plotting the Q(y) relations from Table 1, then reading the graph for depth as a function of Q_{tot}, and converting to spread.

Table 2: Empirical coefficients for head-discharge relationships, SI units. Ranges are the same as for Table 1.

Sump conditions: constants for the cubic relationship $y(Q)=b_1+b_2Q+b_3Q^2+b_4Q^3$

Case	b_1	b_2	b_3	b_4
L=150 mm	0.0	24.2	10.	-0.57
L=790 mm	0.0	-1000.	-540.	83.00
L=790 mm	0.0	1.44x10^5	1.09x10^4	4.43

Note: The coefficients in this table cannot be extrapolated to other size apertures.

CONCLUSIONS

1. The hydraulic performance of rectangular drains formed in concrete barrier walls has been measured under sump conditions and also for a range of face velocities. It was found that depth of the main flow near the inlet entrance could be used as a reliable predictor of discharge.

2. Curved edge inlets were tested for both sump and flows with face velocity, in an attempt to better understand the changes in performance caused by accidental chipping or deliberated streamlining of the inlet face. Substantial improvements were noted only for the sump flows.

3. For design purposes, several empirical correlations for discharge as a function of head have been presented. Conventional correlations[4] could also be used with caution.

4. Both a detailed and approximate computational schemes to analyze the multiple inlet problem presented by a barrier wall has been developed and several example cases have been discussed. A simplified application technique is suggested as an adequate method for spread prediction, without requiring extended computations.

5. Although the smaller inlets appear to perform better than the larger inlets, the capacity of a single large inlet is superior, and barrier blocks with this configuration should be installed if possible. With regard to improving the drainage capacity of barrier wall systems, a number of options were considered. The most promising approach is to incorporate larger openings (length but not necessarily height) at the base of each block. As recutting existing openings is probably impractical, sizing could be changed as blocks are replaced. Certainly the entrance edges should be rounded in any new design. These new designs

could be applied in regions with substantial problems initially, as a part of a long term replacement strategy.

6. Clogging of the drain openings may pose a special problem due to the small vertical clearance and long passage. No data was taken representative of trash accumulation, however it is suggested that trial calculations can be made by assuming that a portion of the apertures are completely blocked.

REFERENCES

1. Roadway and Traffic Design Standards, Florida Department of Transportation, 1996.

2. Robinson, D.I., and McGhee, T.J., "Computer Modeling of Side-Flow Weirs", J.Irrigation and Drainage Engineering, Vol 119, No. 6, Nov./Dec. 1993

3. Singh, R. and Satyanarayana, T., "Automated Field Irrigation System Using Side Weirs", J.Irrigation and Drainage Engineering, Vol. 120, No. 1, Jan./Feb., 1994

4.Johnson, F. L. and Chang, F.M., Drainage of Highway Pavements HEC 12, FHWA, 1984.

5. Young, G.K., Walker, S.E., and Chang, F., Design of Bridge Deck Drainage, HEC 21, FHWA, 1993.

6. Hotchkiss, R. H. Bohac, D. E. and Truby, J., "New Lessons about the Hydraulic Performance of Highway Storm Sewer Inlets", Hydraulic Engineering , Proceedings of the 1991 Conference, Shane, R. M., ed., ASCE, pp. 102-108, 1991.

7. Henderson, F.M. Open Channel Flow, Macmillan Co., New York, N.Y., 1966.

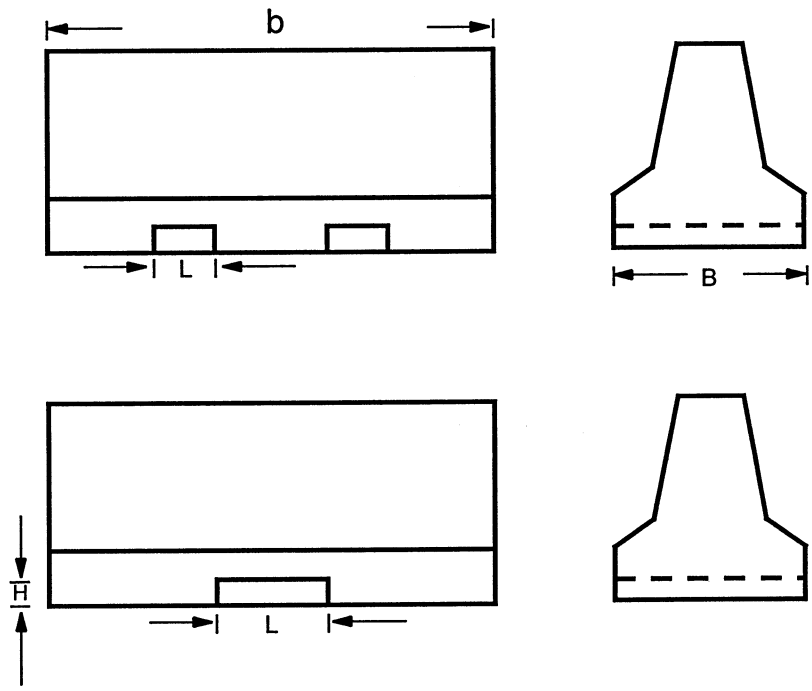

Figure 1: Configuration and notation for barrier wall blocks with flow inlets for drainage.

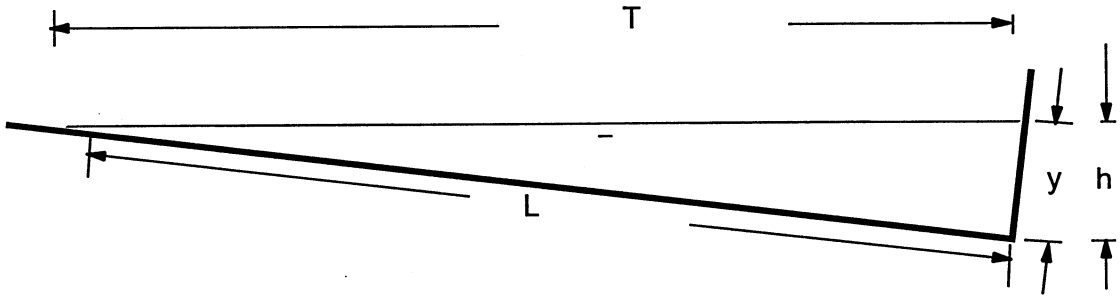

Figure 2: Notation for flow in a simple triangular flow channel.

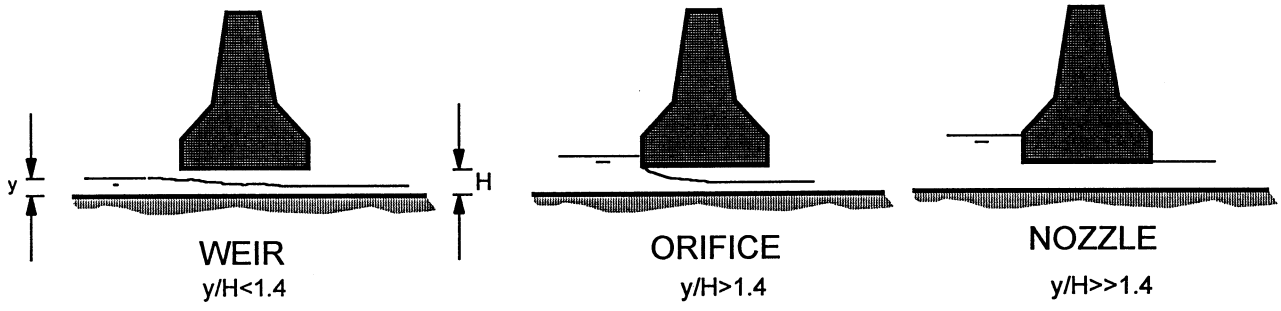

Figure 3: Illustration of several possible flow modes for inlets.

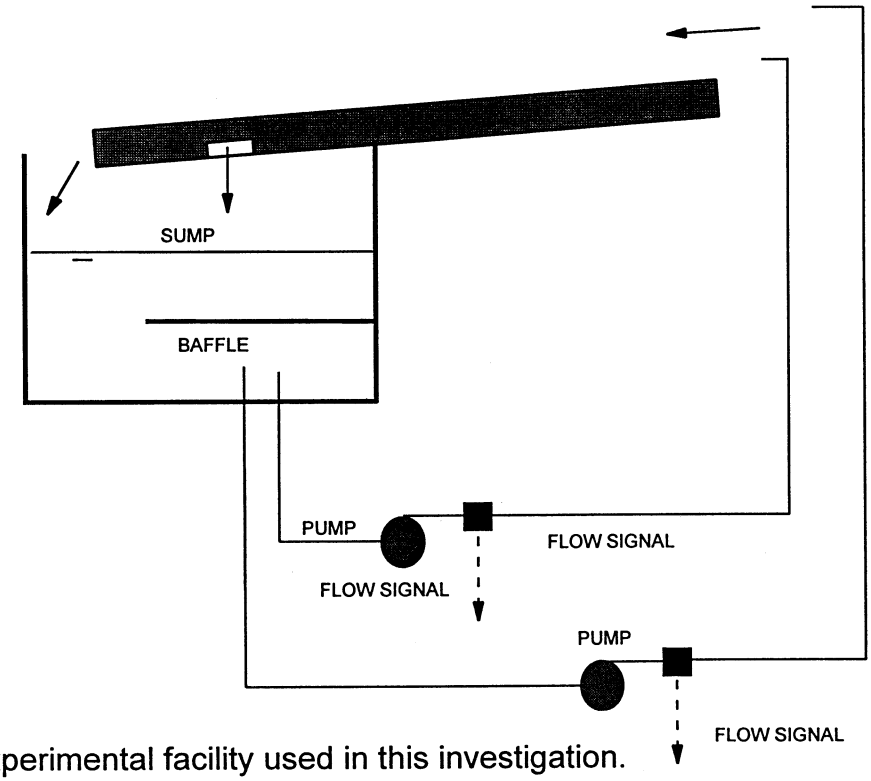

Figure 4: Experimental facility used in this investigation.

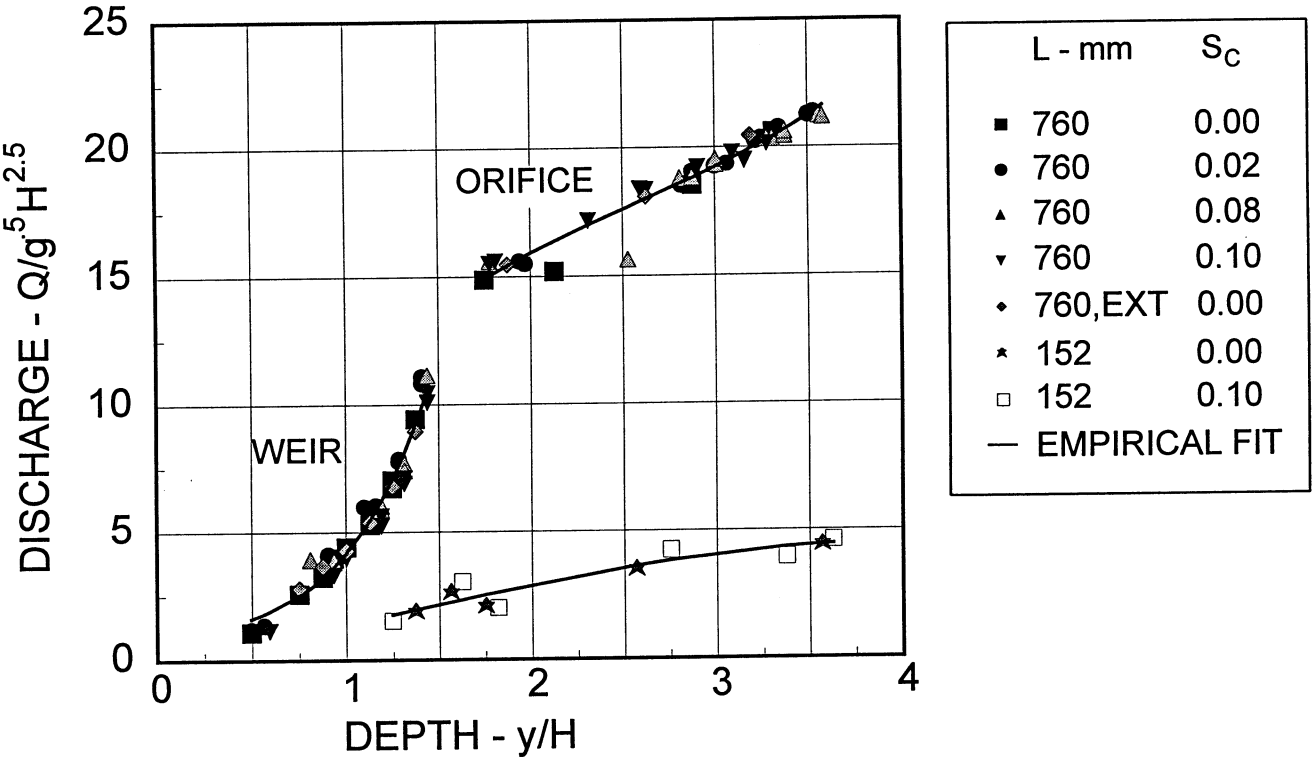

Figure 5: Discharge data and empirical data for inlet performance under sump conditions.

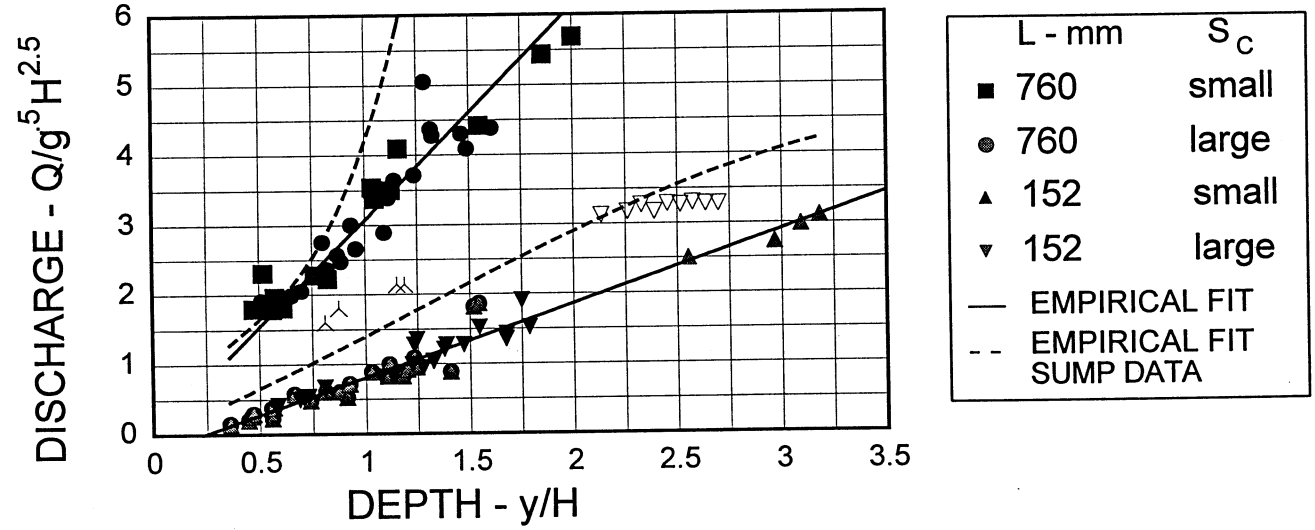

Figure 6: Discharge data and empirical relationships for inlets with transverse flow conditions past the inlet face (the inverted "Y" represents data for which calibration of the flow measurement was questionable).

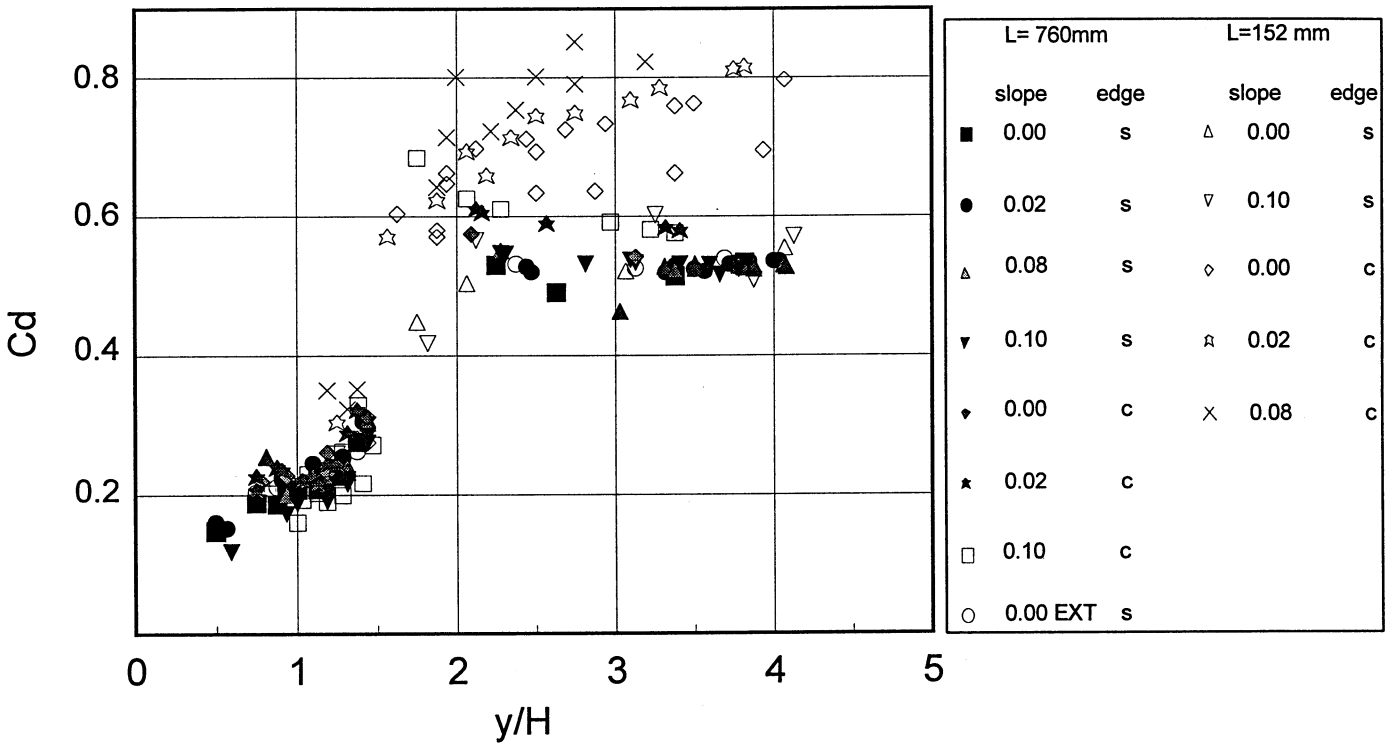

Figure 7: Coefficient of discharge for various configurations at sump conditions. The edge condition is represented by "s" for sharp and "c" for rounded.

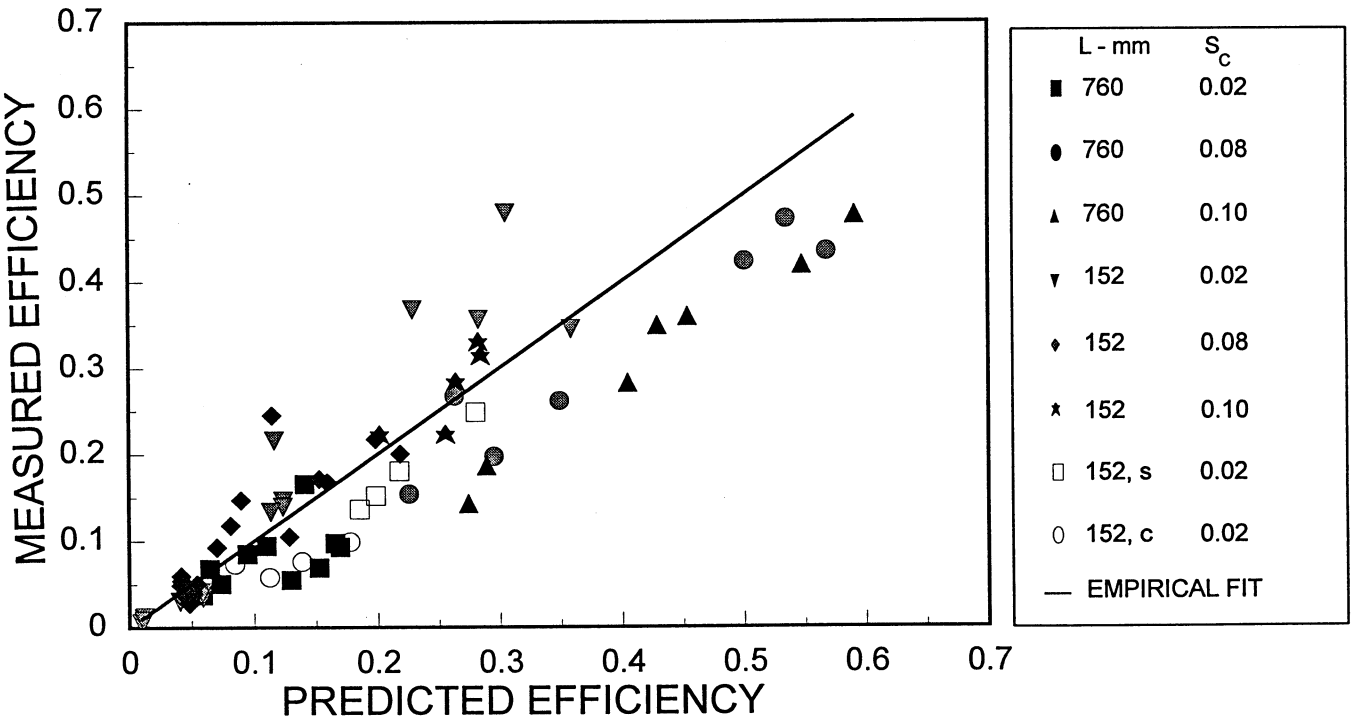

Figure 8: Efficiency comparisons for inlet performance with transverse flow conditions (cf. Reference 4).

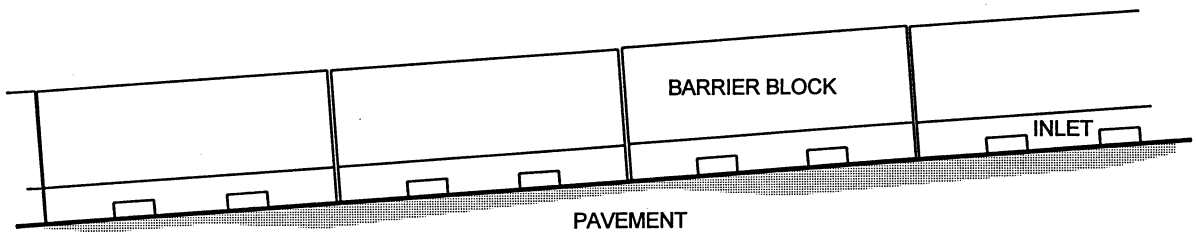

Figure 9: Configuration of a line of barrier blocks placed on grade.

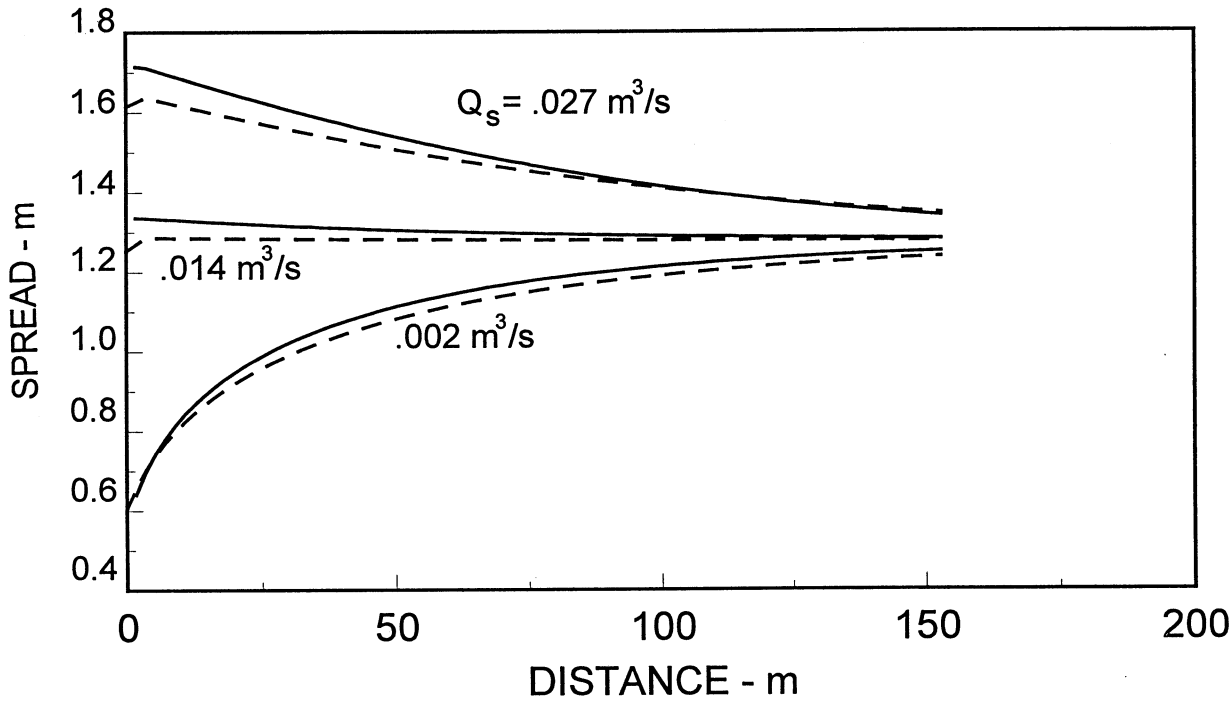

Figure 10: Modeling of spread along a line of barrier blocks for three different initial flows, Q_s. Solid lines denote numerical solution, dashed lines indicate approximate solution.

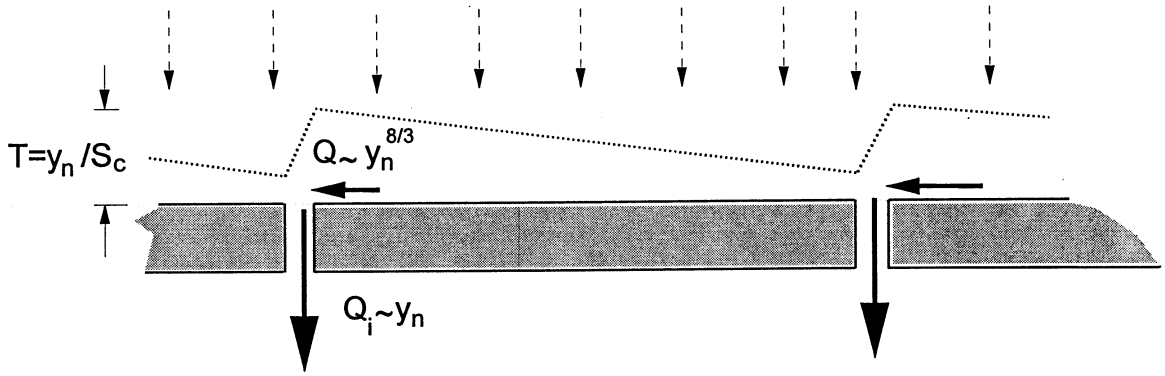

Figure 11: Illustrating the flow and spread condition developed between inlets.

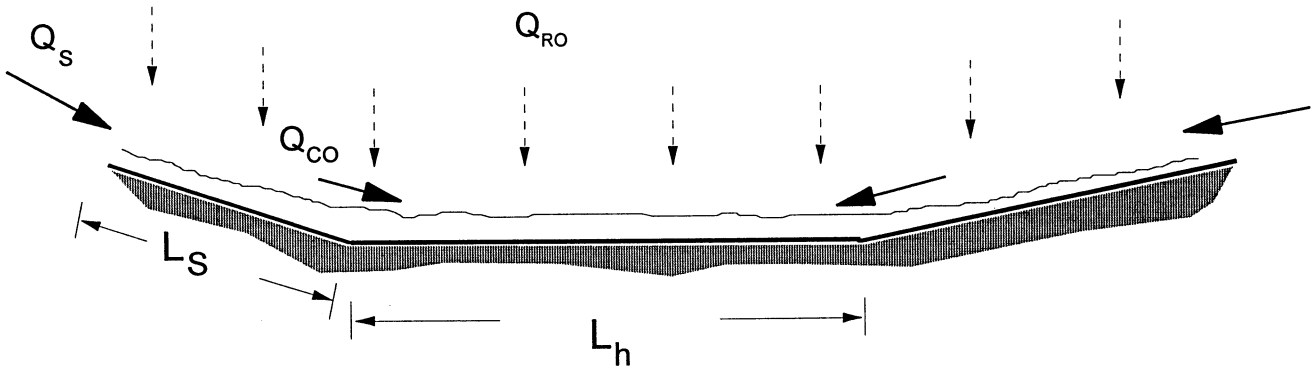

Figure 12: Example of a barrier wall system. Note carryover flow to horizontal section from flanking slopes.